Robust Facility Location for United Nations High Commissioner for Refugees

15.094 Robust Optimization, Final Report

Kayla S. Cummings
kaylac@mit.edu

Josh T. Wilde
jtwilde@mit.edu

Executive Summary

1 Context

Network configuration is the first determinant for a nimble and cost-effective humanitarian supply chain. In order to meet ongoing and emergency demand, humanitarian organizations seek optimal strategies to preposition relief items near disaster-prone areas [1]. In particular, United Nations High Commissioner for Refugees (UNHCR) has identified 11 candidate global warehouse locations for their supply chain, 7 of which are already open. We discuss how UNHCR should select their warehouse locations to meet the needs of 69 million forcibly displaced people in 138 countries [2].

2 Summary of Methods

Our model decides the network configuration based on second-stage decisions about inventory preposition and anticipated flows from warehouses and suppliers to demand outposts, with the dual objective of minimizing both network configuration costs and lead times. Our main contribution is to model highly uncertain demand for emergency humanitarian aid using robust optimization. The emergency relief context is particularly complex, because demand can wildly oscillate between negligible and astronomical levels from year to year. This factor indicates that historical demand is not the best predictor of future demand in the context of humanitarian facility location, and also challenges us to formulate an uncertainty set that is not too conservative.

We meaningfully constrain our uncertainty using machine learning demand forecasts for the pre-planning period. Our forecasts supply us with rough regional bounds on emergency demand that we can shrink and grow in accordance with the confidence we wish to capture in our model. Further, we explicitly embed the trade-off between relying on history and looking forward by parameterizing our trust in the forecast, using average historical demand as a regularization term.

3 Recommendation and Discussion

In Table 1, we juxtapose our recommendation with the proposal from Jahre *et al.* and the current UNHCR facility locations [3]. Our model consistently returns the listed facilities as well as Denmark, with very little variability; our model never indicates significant inventory needs in Denmark, so we recommend its closure to simplify the supply chain.

Country	Cameroon	Denmark	Djibouti	Ghana	Jordan	Kenya	Malaysia	Pakistan	Spain	Tanzania	UAE
C., W.	**X**		**X**	**X**	**X**	**X**	**X**		**X**		
Current	X	X		X	X	X				X	X
Jahre [3]	X		X	X	X		X		X	X	X

Table 1: Current and recommended network configurations.

Our network configuration is reasonably stable and conservative, despite inventory pre-positioning that is predictably paranoid and highly sensitive to the specific uncertainty set. We claim that our recommendation gives UNHCR the potential to adequately respond to any global emergency that might reasonably occur. Robust optimization and machine learning cooperate to enhance UNHCR supply chain resilience.

Technical Summary

Section 1 describes the nominal model [3], UNHCR data, demand forecasting models, uncertainty set construction based on demand forecasts, our robust model, and the formulation of tractable robust counterparts. Section 2 compares our robust results with Jahre's. We also evaluate the impact of the confidence level we capture and the trust we place in our uncertainty sets, as well as the demand forecast point estimates themselves. Finally, Section 3 concludes with implications and next steps.

1 Methods

We extend work by Jahre *et al.* [3], whose UNHCR warehouse location model incorporates parameterized contextual factors such as co-location, safety, pilferage, and accessibility in order to design a merged supply chain for emergency relief and ongoing operations. Our work also intersects with literature related to humanitarian aid demand forecasts, data-driven optimization, robust facility location, and robust multi-objective optimization. Van der Laan and colleagues forecasted humanitarian relief demand at the product level for smaller relief efforts [4], while we forecast country-level emergency needs for all non-perishable items that UNHCR provides. Work in data-driven robust optimization motivates our strategy for constructing uncertainty sets from these data-driven forecasts [5]. Baron, Milner, and Naseraldin demonstrate that adding robustness to protect against demand uncertainty in facility location problems can yield both meaningfully different network designs as well as significant improvements in solution quality [6]. We utilize the results from Doolittle to justify the construction of a Pareto front of robust efficient solutions in our multi-objective setting [7]. Yahyaei and Bozorgi-Amiri analyze the impact of robustness on a national humanitarian relief network [8], but they do not use data-driven forecasts to construct their uncertainty sets.

Our first contribution is to propose a framework for UNHCR to make facility location decisions that incorporate both historical and forecast demand scenarios and parameterizes relative trust in these scenarios. Our second contribution is to validate under uncertain demand the strategic facility location decisions that [3] propose and recommend a separate short-term modeling framework for periodic inventory allocation.

1.1 Data

Tina Rezvanian, a coauthor of [3], provided country-level emergency response and ongoing operations demand in USD for 2011-2013; estimated lead times and transportation costs between demand outposts, warehouse locations, and global suppliers; fixed and variable costs of opening warehouses; warehouse inventory capacities and stocking costs; and public covariate data necessary for demand classification forecasts. After cleaning and standardizing the data, we were able to approximately replicate Jahre's results [3].

1.2 Model

Our model (1) supplies upper and lower bounds for emergency demand at a regional level, with regions defined by the United Nations Statistics Division classification [9]. After (2) converting the forecasts into country-level box uncertainty sets, we (3) solve the tractable robust counterpart of a robust-friendly nominal reformulation of Jahre's model [3].

1.2.1 Emergency Response Demand Forecasts

The incorporation of demand forecasts into a robust humanitarian supply chain model precludes unreasonably expensive network designs [10]. We use both regression and classification to produce the forecasts. In the former, we predict three-month average emergency demand in USD from selected covariates. In the latter, we assign to each region a probability distribution over a set of five discrete classes of emergency demand. By forecasting at a regional level rather than a country-level, we assume that countries in the same region have highly correlated demand. Tina Rezvanian provided us with her current classification forecasts, and we leveraged her identification of meaningful covariates to build our own ordinary least squares regression model. The goal of the demand forecasting exercise is to generate an interval range of emergency demand for the six regions with nonzero historical emergency demand in our data.

Classification Forecasts. The classification model assigns a probability to the five classes of emergency demand listed in Table 2 for each region. We take the classification results directly from Tina Rezvanian without adjustment. The independent variables in the classification model include historical emergency and ongoing UNHCR demand,

counts of refugees and other types of forcibly displaced persons from UNHCR, counts of battle-related deaths from the Uppsala Conflict Data Program, and political instability indices from the European Commission. The dependent variable is 3-month average emergency demand in USD.

Demand (USD)	Europe			Asia					Africa				
	W	S	E	W	S	Cen.	SE	E	W	S	Mid.	E	N
0–10^5	0.74	0.08	0.58	0.02	0.18	0.88	0.65	0.98	0.13	0.87	0.1	0.02	0.26
10^5–10^6	0.03	0.04	0.04	0	0.13	0.11	0.05	0.01	0.19	0	0.07	0.01	0.04
10^6–$5 \cdot 10^6$	0.12	0.26	0.18	0.02	0.31	0.01	0.05	0.01	0.42	0.01	0.33	0.08	0.2
$5 \cdot 10^6$–10^7	0.05	0.32	0.08	0.03	0.3	0	0.04	0	0.19	0.01	0.36	0.09	0.28
10^7–$5 \cdot 10^7$	0.06	0.3	0.12	0.93	0.08	0	0.21	0	0.07	0.11	0.14	0.8	0.22

Table 2: Preliminary demand classification forecasts.

Regression Forecasts. We estimate an ordinary least squares (OLS) regression based on the same potential covariates and dependent variable. Many of the potential covariates are highly correlated (0.5-0.8) and provide statistically redundant information, so our final OLS formulation predicts current emergency demand based only on the prior year's count of battle-related deaths. The regression explains about half of the variance of emergency demand, and the fit of the model could almost certainty be improved with access to a longer time series of emergency demand data. We chose an ordinary least squares model because the structure provides access to well-understood, closed-form prediction intervals based on the standard error of the regression. Closed-form prediction intervals do not exist for more complex general linear approaches for modeling non-negative data, such as negative binomial regression.

Demand (10^3 USD)	Eur.			Asia					Africa				
	W	S	E	W	S	Cen.	SE	E	W	S	Mid.	E	N
Pred. Value	143	127	465	10,876	15,906	153	2,388	131	3,213	127	5,334	3,004	1,919
Std. Error	564	565	543	1,746	2,608	563	541	564	602	565	859	584	521

Table 3: Preliminary linear regression demand forecasts.

1.2.2 Uncertainty sets

Algorithm 1 maps regional classification forecasts to regional uncertainty sets. We first select $\theta \in [0, 1]$ so that we are at least $\theta\%$ confident that the uncertainty set for each region $r \in R$ captures future emergency response demand. If there are C ordered classes, then p_{rc} is the predicted probability that region $r \in R$ will require emergency aid in the range $[d_c^L, d_c^U]$ USD for class $c \in \{1, \ldots, C\}$. The algorithm takes our confidence level and forecasts as input, and initializes by selecting the likeliest demand class as each region's uncertainty set. We greedily absorb the likeliest adjacent demand class into the interval until the collectively covered probability exceeds the required confidence level.

Algorithm 1 Convert regional classification forecasts to regional uncertainty sets

procedure CONVERT(θ, $p[r \in R, c \in \{1, \ldots, C\}]$)
  $L[r \in R] \leftarrow 0$; $U[r \in R] \leftarrow 0$
  $p[r \in R, 0] \leftarrow 0$; $p[r \in R, C+1] \leftarrow 0$ // Clean up edge cases
  for $r \in R$ **do**
    $B \leftarrow \left\{\arg\max_{c \in \{0,\ldots,C+1\}} \{p_{rc}\}\right\}$ // Demand classes included in uncertainty set
    $p \leftarrow p[r, B[0]]$
    while $p < \theta$ **do**
      $B \leftarrow B.\text{append}\left(\arg\max_{d \in \{\min(B)-1, \max(B)+1\}} p_{rd}\right)$
      $p \leftarrow \sum_{b \in B} p_{rb}$
    $L[r] \leftarrow d^L_{\min(B)}$; $U[r] \leftarrow d^U_{\max(B)}$
  return $(L[r \in R], U[r \in R])$

We map regional regression forecasts to regional uncertainty sets using expressions (1) and (2), where $\hat{d}_r^{ER}$ is the predicted value for emergency demand for region r, SE is the standard error of the regression model, and η is a confidence parameter that controls the size of the prediction interval.

$$L_r = \max\left(0, \hat{d}_r^{ER} - \eta SE\right) \tag{1}$$

$$U_r = \hat{d}_r^{ER} + \eta SE \tag{2}$$

We set $\eta = 1$ in our results; with more data, this parameter could be set through cross-validation.

Based on these forecast intervals, our initial uncertainty set is given by (3).

$$\mathcal{U} = \bigcup_{r \in R} \mathcal{U}_r = \bigcup_{r \in R} \left\{ d^{ER} \,:\, d_j^{ER} \in [L_r, U_r],\ j \in A_r \right\} \tag{3}$$

Our adversary always hands us the worst case scenario in a robust optimization regime. In particular, our uncertainty set includes the case that $d_j^{ER} = U_r$ for each $r \in R$ and $j \in A_r$. Guarding against this unlikely realization will result in an unrealistically conservative solution. Thus, we convert from regional uncertainty sets $\mathcal{U}_r$ to country-level bounds, as follows.

We predict each country's share of regional emergency demand in equation (4) based on its average historical share of emergency demand within its region.

$$\alpha_j^r = \frac{\bar{d}_j^{ER}}{\sum_{k \in A_r} \bar{d}_k^{ER}}, \qquad r \in R, j \in A_r \tag{4}$$

We scale the range of emergency demand for country j by α_j^r. We capture trust in the forecasting model according to parameter $\beta \in [0, 1]$, defaulting to average historical emergency demand when $\beta = 0$.

$$L_j = \beta \cdot \alpha_j^r L^r + (1 - \beta) \cdot \bar{d}_j^{ER}, \qquad r \in R,\, j \in A_r \tag{5}$$

$$U_j = \beta \cdot \alpha_j^r U^r + (1 - \beta) \cdot \bar{d}_j^{ER}, \qquad r \in R,\, j \in A_r \tag{6}$$

Thus, our final uncertainty set is given by (7).

$$\mathcal{U} = \bigcup_{j \in A} \left\{ d^{ER} \,:\, d_j^{ER} \in [L_j, U_j] \right\} \tag{7}$$

1.2.3 Reformulation of Jahre's model into our robust model

Jahre's model is a dual-objective, two-stage stochastic program. We open facilities in the first stage based on second-stage inventory pre-positioning and projected flows from global warehouses and suppliers to coarsely anticipated demand points. Two objective functions minimize the expected costs of configuring the network and the expected lead times. See [3] for the full formulation.

Here we reproduce the objective function and constraints in [3] related to emergency demand. Table 4 itemizes all model components.

$$\begin{aligned} \min \sum_{g \in G} f_g y_g + \sum_{g \in G, s \in S} C_{sg} z_{sg} + \sum_{g \in G} v_g I_g + \sum_{k \in K, j \in A} \alpha_k \Big(\big(\sum_{g \in G} C_{gj}^{oo} x_{gj}^{oo,k} + \sum_{s \in S} C_{sj}^{oo} x_{sj}^{oo,k} \big) d_j^{oo,k} + \\ \sum_{g \in G} \left((C_{gj}^{ER} x_{gj}^{ER,k})((1 - \gamma_j^k) lim + d_j^{ER,k} \gamma_j^k) + (CL_{gj}^{ER} ex_{gj}^{ER,k} (1 - \gamma_j^k)(d_j^{ER,k} - lim)) \right) \Big) \end{aligned} \tag{8}$$

$$\sum_{g\in G}(x_{gj}^{ER,k}d_j^{ER,k} + ex_{gj}^{ER,k}d_j^{ER,k}) = d_j^{ER,k} \qquad j \in A \tag{9}$$

$$\sum_{g\in G} x_{gj}^{ER,k}d_j^{ER,k} = (1-\gamma_j^k)lim + d_j^{ER,k}\gamma_j^k \qquad k \in K, j \in A \tag{10}$$

$$\sum_{g\in G} ex_{gj}^{ER,k}d_j^{ER,k} = (1-\gamma_j^k)(d_j^{ER,k} - lim) \qquad j \in A, k \in K \tag{11}$$

$$\sum_{j\in A}(x_{gj}^{oo,k}d_j^{oo,k} + x_{gj}^{ER,k}d_j^{ER,k} + ex_{gj}^{ER,m}d_j^{ER,k}) \leq 43000I_g \qquad k \in K, g \in G \tag{12}$$

The objective function minimizes the total cost of opening the warehouses, stocking inventory, and transporting goods to the demand points. Constraint (9) ensures emergency demand is satisfied. Constraints (10) and (11) prioritize air shipment of emergency demand up until the UNHCR limit of 10 TEUs (equivalent to 430,000 USD), shipping remaining demand using cheaper but slower express land and sea routes. Constraint (12) enforces inventory limits for each warehouse in USD.

We reformulate the Jahre's model to obtain a robust model whose associated robust counterpart will be tractable. We first substitute quantities for proportions into the model, thereby disposing of an implicit, sub-optimal linear decision rule. As a result, we automatically eliminate uncertain parameters from the objective function (8) and constraint (12). Now we can convert constraints (9), (10), and (11) into inequalities.

We augment the uncertainty set in equation (13).

$$\hat{\mathcal{U}} = \left\{(d^{ER}, z) \,:\, d_j^{ER} \in \mathcal{U}, z_j \leq d_j^{ER}, z_j \leq lim, j \in A\right\} \tag{13}$$

Then we reformulate as follows, noting that only two constraints contain uncertain parameters.

$$\sum_{g\in G} w_{gj}^{ER} \leq lim \qquad j \in A \tag{14}$$

$$\sum_{g\in G} w_{gj}^{ER} \geq z_j \qquad j \in A,\ (d_j^{ER}, z_j) \in \hat{\mathcal{U}} \tag{15}$$

$$\sum_{g\in G}(w_{gj}^{ER} + ew_{gj}^{ER}) \geq d_j^{ER} \qquad j \in A,\ (d_j^{ER}, z_j) \in \hat{\mathcal{U}} \tag{16}$$

We reformulate the constraints so their robust counterparts accomplish the same goals as Jahre's formulation, while minimizing the number of constraints with uncertain parameters. If emergency demand exceeds 10 TEUs, then constraints (14) and (15) work together to ensure we send 10 TEUs by air. Otherwise, constraint (15) works with the cost-minimizing objective function to ensure we only send the requested amount of emergency demand by air. Constraint (16) ensures we send excess emergency supplies using express land shipment. Constraints that do not involve uncertain parameters, including flow conservation and warehouse capacity constraints, are not enumerated here.

We compute the dual-objective Pareto frontier using the same approach as Jahre *et al.* [3]. To do so, we implement a robust minimum-lead-time model with a budget constraint that allows us to deviate by at most ϵ from our robust-optimal network configuration cost. We approximate the Pareto frontier by incrementing ϵ and re-solving the budgeted lead-time model. We interpret this Pareto front differently in a robust context. It is the "best-worst-case" Pareto frontier: we have computed the best we can do in every worst-case scenario that we have modeled. Together with the nominal Pareto frontier, we quantify the cost of achieving a particular lead time if we want to protect against uncertainty. *Honestly, we struggled to justify this approach theoretically: we would particularly appreciate feedback on this part of the project as we move forward.*

1.2.4 Robust counterpart

We present the tractable robust counterparts of constraints with uncertain parameters in our robust minimum cost model.

$$\sum_{g \in G} (w_{gj}^{ER} + ew_{gj}^{ER}) \geq \bar{d}_j^{ER} + \beta \cdot (\alpha_j^r U^r - \bar{d}_j^{ER}) \qquad j \in A \tag{17}$$

$$\sum_{g \in G} w_{gj}^{ER} \geq lim \qquad r \in R,\, j \in A_r \,:\, \beta \geq \frac{lim - \bar{d}_j^{ER}}{\alpha_j^r U^r - \bar{d}_j^{ER}} \tag{18}$$

$$\sum_{g \in G} w_{gj}^{ER} \geq \bar{d}_j^{ER} + \beta \cdot (\alpha_j^r U^r - \bar{d}_j^{ER}) \qquad r \in R, j \in A_r \,:\, \beta < \frac{lim - \bar{d}_j^{ER}}{\alpha_j^r U^r - \bar{d}_j^{ER}} \tag{19}$$

Proof. Constraint (16) is equivalent to the following.

$$\sum_{g \in G} (w_{gj}^{ER} + ew_{gj}^{ER}) \geq \max_{d_j^{ER} \in \hat{\mathcal{U}}} d_j^{ER} = \bar{d}_j^{ER} + \beta \cdot \left(\alpha_j^r U^r - \bar{d}_j^{ER}\right) \tag{20}$$

The inequality holds for all $d_j^{ER} \in \hat{\mathcal{U}}$ if and only if it holds for the maximum. Equation (6) explains the last equality.

Now consider constraint (15).

$$\sum_{g \in G} w_{gj}^{ER} \geq \max_{z_j \in \hat{\mathcal{U}}} z_j = \min\left\{d_j^{ER}, lim\right\} = \min\left\{U_j, lim\right\} = \min\left\{\bar{d}_j^{ER} + \beta \cdot (\alpha_j^r U^r - \bar{d}_j^{ER}), lim\right\} \tag{21}$$

An adversary hands us the maximum value of z_j, which is the minimum of its two upper bounds. If the minimum happens to be d_j^{ER}, then the adversary will hand us the highest possible value, which is the upper bound on d_j^{ER}.

Suppose the minimum is lim. Then we obtain the condition in equation (18) from $lim \leq \bar{d}_j^{ER} + \beta \cdot (\alpha_j^r U^r - \bar{d}_j^{ER})$. Otherwise, we obtain constraint (19).

□

The β parameter acts as a safety term that governs the level of conservatism in the model. However, the relationship between β and the level of conservatism can differ for each country j depending on the sign of $\alpha_j^r U^r - \bar{d}_j^{ER}$. We develop this relationship further in Section 2.3.

Instances of the robust mixed integer linear program had a maximum of 19,217 variables and 7,266 constraints. All instances were all solved within seconds using JuMP [11] and Gurobi 8.0 [12] on a MacBook Pro with 16 GB of RAM.

2 Results and Discussion

Computational results focus on the robust model with uncertainty sets derived from the classification model. We set our confidence level at $\theta = 0.5$, and our final uncertainty set places 50% weight on the forecast bounds and 50% weight on historical average demand. Later, we analyze effects of confidence and trust.

2.1 Nominal vs. Robust: Stable network configuration and volatile inventory allocation

Figure 2 juxtaposes nominal and robust network configurations. In the example, forecasted worst-case demand in North and East Africa is substantially higher than historical realizations. In spite of this, the robust and nominal solutions both choose to open the same eight warehouses–Denmark, Jordan, Ghana, Cameroon, Kenya, Spain, Malaysia, and Djibouti–leaving Tanzania, UAE, and Pakistan closed.

Rather than opening additional warehouses, the robust model stocks 42% more inventory than the nominal model and reallocates this inventory to regions that are initially counterintuitive. For example, in the nominal solution there are no meaningful flows from the warehouse in Spain. In the robust solution, Spain becomes a network hub, controlling an

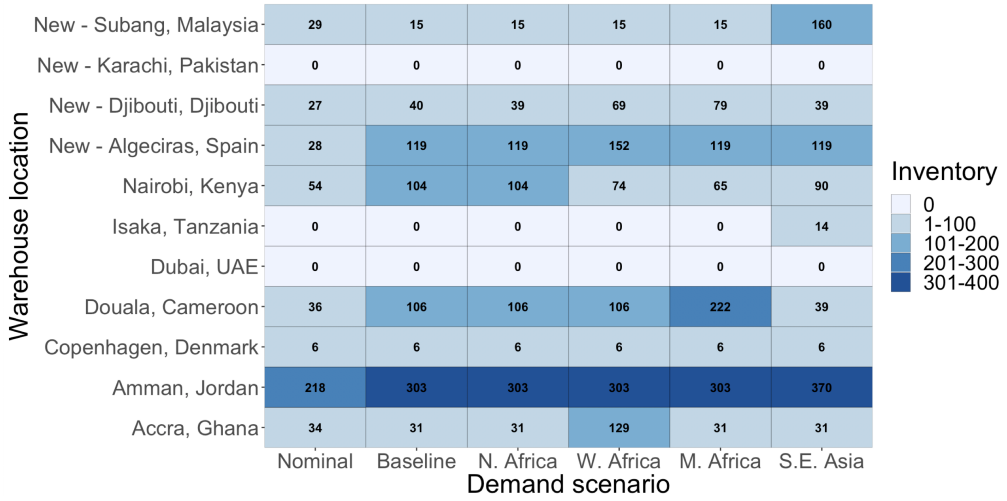

Figure 1: Inventory levels for nominal solution vs. various robust solutions. Baseline solution uses uncertainty set based on classification forecast with $\theta = \beta = 0.5$. We select $\epsilon = 0.05$ from the corresponding solution's position on the Pareto front in Figure 4b. Other scenarios shock the corresponding regions with worst-case ER demand equivalent to that of Eastern Africa.

incremental 10% of total global inventory. Spain is a low cost supplier to both African regions with highly uncertain demand, and the robust configuration map indicates meaningful flows from Spain to both Tanzania and Tunisia. On a relative basis, Malaysia and Jordan are allocated a smaller proportion of global inventory in the robust design because these warehouses are supplying regions with lower or less volatile demand (Figure 3a).

In addition to analyzing the network configuration under our current classification forecast, we also introduce alternative forecast scenarios corresponding to demand shocks in other regions. We permuted the country uncertainty set bounds, simulating possible alternative demand forecasts to test the resilience of our original solution. Surprisingly, we found that the network configuration did not change in any of the alternative forecast scenarios. Instead of open-

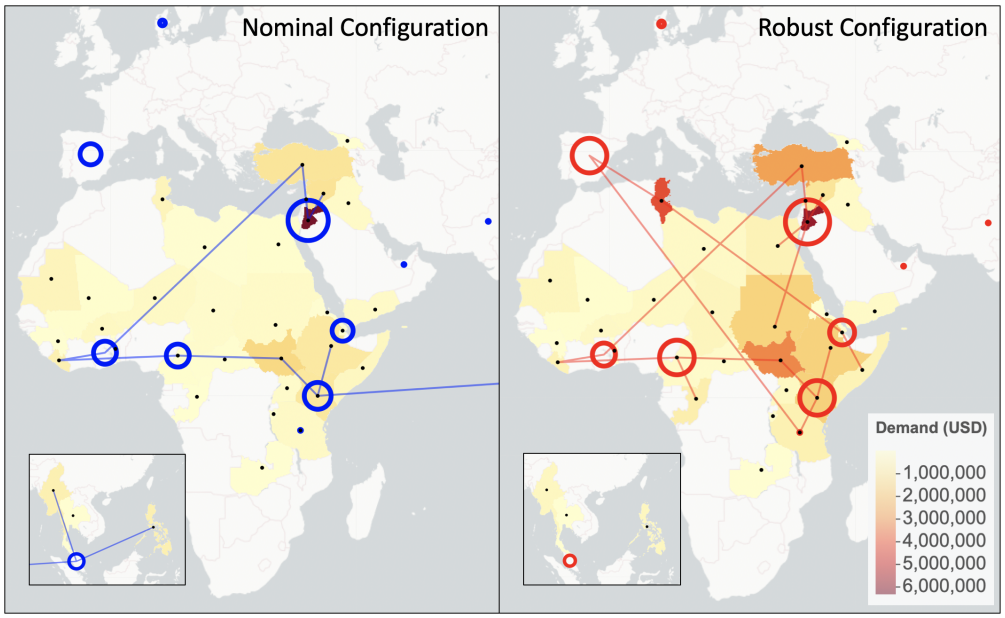

Figure 2: Nominal network configuration vs. robust network configurations based on classification forecasts, with $\theta = \beta = 0.5$ and $\epsilon = 0.05$. The radii of the hollow colored circles indicate inventory levels at warehouse locations. Black dots are demand outposts. Included flows exceed 50,000 USD.

(a) Comparison of nominal and robust inventory allocation in Figure 2.

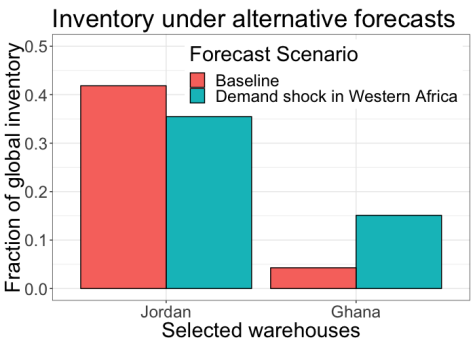

(b) Comparison of inventory allocation among selected scenarios from Figure 1.

Figure 3: Selected relative differences in proportions of inventory allocation across different models.

ing different warehouses, the optimal response to varying the demand forecast is to significantly reallocate inventory among the eight warehouses. Figure 3 provides an example of this reallocation under an alternative forecast with very high demand in Western Africa. Uncovering this surprising stability in the network configuration, as well as the extreme sensitivity of inventory allocation to the demand forecast, was a key benefit of employing the robust approach with demand forecasts.

2.2 Quantifying the added benefit of forecasting and robustness

Fixing the facility locations and inventory allocations from the robust and nominal models, we simulated 100 demand scenarios to quantify the added benefit of robustness and forecasting. For each scenario we sampled uniformly at random from each country's uncertainty set and used secondary models to measure fulfillment deficiency and fulfillment cost for the two models. The deficiency model defines an auxiliary, uncapacitated "warehouse" with flows to all demand points. We minimize all flows from the auxiliary warehouse, interpreting the optimal solution as a lower bound on the fulfillment deficiency of the network configuration and inventory allocation. The fulfillment cost model computes minimum shipping costs with the same air and land shipment priorities, which gives us a lower bound on the cost of fulfilling both ongoing demand and simulated emergency demand for the specified inventory levels.

By construction, the robust inventory allocation does not have any fulfillment deficiency under the scenarios that we tested, while the nominal model is unable to fulfill USD 2.3 million of demand in the median simulation. In addition, median fulfillment cost is nearly USD 2 million lower for the robust allocation compared to the nominal.

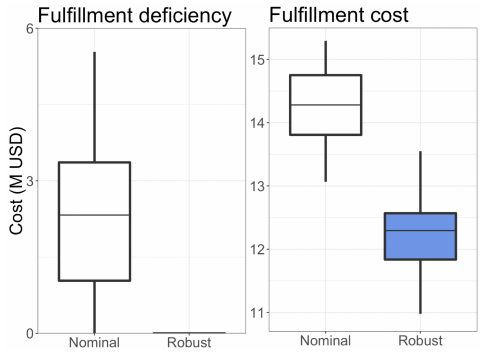

(a) Robustness improves demand fulfillment capabilities and decreases realized fulfillment costs.

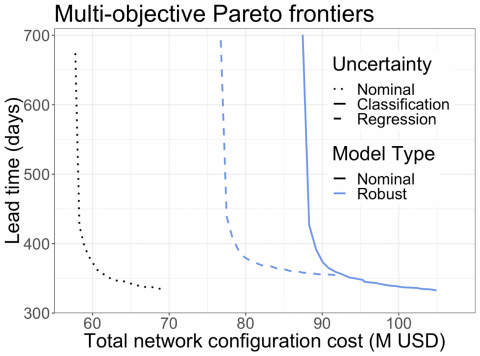

(b) The price of robustness is a substantial increase in network configuration costs.

Figure 4: Quantifying differences between nominal and robust optimal solutions.

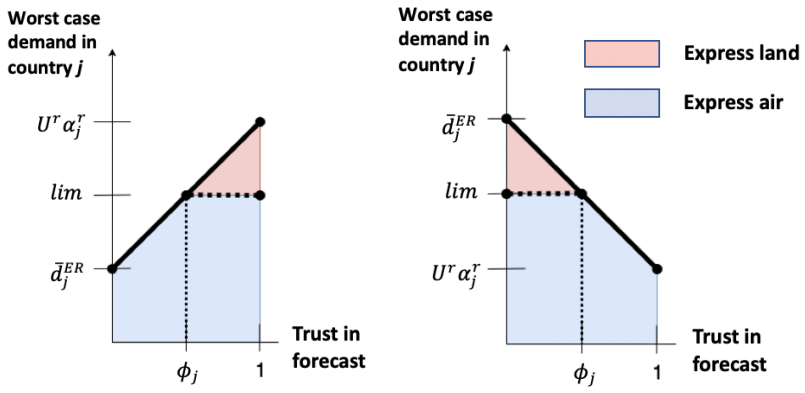

(a) $U^r\alpha_j^r > \bar{d}_j^{ER}$ (b) $U^r\alpha_j^r < \bar{d}_j^{ER}$

Figure 5: If $0 < \phi_j < 1$, express land shipment is necessary to fulfill the fraction of emergency demand above lim. The red area represents this fraction.

Figure 4a indicates that the robust solution incurs a substantial increase in additional inventory cost to eliminate fulfillment deficiencies and reduce fulfillment costs. While this substantial additional inventory investment is likely not reasonable for UNHCR, the simulation results hint at the potential benefits of a robust inventory allocation model with uncertainty sets constrained by more accurate demand forecasts.

2.3 Reconciliation of forecasts with history

The trust we place in our demand forecast impacts uncertainty set conservativism. Figure 5 illustrates the relationship between total emergency demand for country j as a function of β, as governed by the robust counterpart in equation (17). The relationship is always linear, but the slope of the line depends on the relationship between $\bar{d}_j^{ER}$ and the upper bound of the uncertainty set, $\alpha_j^r U^r$. If the forecast range exceeds historical average demand, then increasing trust in the forecast increases the conservatism of the uncertainty set, but increased trust has the opposite impact when the forecast upper bound falls below historical demand. The relationship between β and express air shipments to country j depends additionally on whether or the express air limit is between the forecast upper bound and historical average demand. This occurs if $0 < \frac{lim - \bar{d}_j^{ER}}{U^r\alpha_j^r - \bar{d}_j^{ER}} < 1$. In Figure 5, we define $\phi_j = \frac{lim - \bar{d}_j^{ER}}{U^r\alpha_j^r - \bar{d}_j^{ER}}$ and show an example when this limit introduces non-linearity in the relationship between β and express air shipments.

3 Conclusions

We formulated a robust optimization model with data-driven uncertainty sets to design UNHCR's supply chain under uncertain emergency demand. In the process of developing the model, we introduced a framework to flexibly incorporate both historical demand scenarios and forecasts in the formulation of uncertainty sets. As a result, we were able to observe that the eight robust optimal warehouse locations did not change when we induced demand shocks that were outside of the scope of the current forecasts. This key result gives us increased confidence in recommending the facility location solutions from our model. Going forward, we are interested in validating this finding once we have more data by building more accurate forecasting models and testing a wider range of potential demand scenarios.

We highlight that inventory allocation was highly sensitive to the forecast. Given the low variance of the facility locations themselves, we suggest divorcing inventory allocation decision from the facility location decision, without detriment to the global welfare of the supply chain. We plan to develop a secondary model for inventory allocation that fixes facility locations and provides a short-term inventory allocation decision. This model could be static and resolved periodically using a folding horizon approach or it could be a multi-stage program with adaptive variables. In either case, the results from our simulations hint at the possibility of making robust inventory allocation decisions that reduce the cost of fulfilling demand without introducing fulfillment deficiency.

4 Acknowledgements

We gratefully acknowledge Tina Rezvanian and Özlem Ergun for UNHCR data and the emergency demand forecasting framework. Additionally, we thank 15.094 TAs Brad Sturt and Jean Pauphilet for their guidance and suggestions, particularly related to incorporating data-driven forecasts into uncertainty set construction.

5 Appendix

	Nominal Model Sets
S	Set of suppliers
G	Set of global warehouses
K	Set of emergency demand scenarios from [3]
A	Set of all demand points, emergency and ongoing
	Robust Model Sets
R	Set of United Nations Statistics Division regions with emergency demand
A_r	Set of all emergency demand points in region $r \in R$
	Nominal Model Parameters
f_g, v_g	Fixed and variable costs of opening $g \in G$
$C_{gj}, CL_{gj}, C_{sg}, C_{sj}$	Transportation costs from $g \in G$ or $s \in S$ to $j \in A$ or $g \in G$ in USD
l_{gj}, lL_{gj}, l_{sj}	Lead times in days from $g \in G$ or $s \in S$ to $j \in A$
$d_j^{ER,k}, d_j^{oo,k}$	Demand for emergency (ER) or ongoing (OO) supplies at $j \in A$ for scenario $k \in K$ in USD
lim	Equal to $430,000$ USD. Maximum USD value of emergency supplies that can be sent by express air.
γ_j^k	1 if $d_j^{ER,k} \leq lim$, 0 otherwise for $j \in A, k \in K$
	Robust Model Parameters
β	Certain. Trust in demand forecast
α_j^r	Certain. Average historical proportion of ER demand for $j \in A$ in $r \in R$
$\bar{d}_j^{ER}$	Certain. Average historical ER demand for $j \in A$ in USD
$\hat{d}_j^{ER}$	Uncertain. Demand for ER supplies at $j \in A$ in USD
z_j	Uncertain. Lower bound on amount of emergency supplies to send by air for $j \in A$ in USD
	Nominal Model Decision Variables
I_g	Integer. Required number of containers to be stocked at $g \in G$ in TEUs
x_{sj}^{oo}, x_{gj}^{oo}	Continuous. Percentage of ongoing demand to send from $s \in S$ or $g \in G$ to $j \in A$
$x_{gj}^{ER}, ex_{gj}^{ER}$	Continuous. Percentage of emergency demand to send by air or land from $g \in G$ to $j \in A$
y_g	Binary. Indicates whether to open $g \in G$
	Robust Model Decision Variables
$w_{gj}^{ER}, ew_{gj}^{ER}$	Continuous. Amount of emergency response demand in USD to send from $g \in G$ to $j \in A$

Table 4: Components of Jahre's model [3] and our model.

References

[1] J. Komrska, L. R. Kopczak, and J. M. Swaminathan, "When supply chains save lives," *Supply Chain Management Review*, vol. 17, no. 1, pp. 42–49, 2013.

[2] "UNHCR - The UN Refugee Agency." Accessed at `https://www.unhcr.org/` on 18 May 2019.

[3] M. Jahre, J. Kembro, T. Rezvanian, O. Ergun, S. J. Hapnes, and P. Berling, "Integrating supply chains for emergencies and ongoing operations in UNHCR," *Journal of Operations Management*, vol. 45, pp. 57–72, 2016. Special Issue on Humanitarian Operations Management.

[4] E. van der Laan, J. van Dalen, M. Rohrmoser, and R. Simpson, "Demand forecasting and order planning for humanitarian logistics: An empirical assessment," *Journal of Operations Management*, vol. 45, pp. 114–122, 2016.

[5] D. Bertsimas, V. Gupta, and N. Kallus, "Data-driven robust optimization," *Mathematical Programming*, vol. 167, no. 2, pp. 235–292, 2018.

[6] O. Baron, J. Milner, and H. Naseraldin, "Facility location: A robust optimization approach," *Production and Operations Management*, vol. 20, no. 5, pp. 772–785, 2011.

[7] E. K. Doolittle, H. L. M. Kerivin, and M. M. Wiecek, "Robust multiobjective optimization with application to internet routing," *Annals of Operations Research*, vol. 271, pp. 487–525, Dec 2018.

[8] M. Yahyaei and A. Bozorgi-Amiri, "Robust reliable humanitarian relief network design: an integration of shelter and supply facility location," *Annals of Operations Research*, pp. 1–20, 2018.

[9] "UNSD - Methodology." Accessed at `https://unstats.un.org/unsd/methodology/m49/` on 18 May 2019.

[10] K. Peters, H. Fleuren, D. Den Hertog, M. Kavelj, S. Silva, R. Goncalves, O. Ergun, and M. Soldner, "The nutritious supply chain: Optimizing humanitarian food aid," *CentER Discussion Paper Series*, 2016.

[11] I. Dunning, J. Huchette, and M. Lubin, "JuMP: A modeling language for mathematical optimization," *arXiv:1508.01982 [math.OC]*, 2015.

[12] Gurobi Optimization, LLC, "Gurobi optimizer reference manual," 2019.